AD-A189 790 SPATIAL MATCHED PROCESSING FOR MULTIPATH PROPAGATION (U) MICHIGAN UNIV ANN ARBOR COMMUNICATIONS AND SIGNAL PROCESSING LAB M A DZIECIUCH ET AL 16 NOV 87 1/1

UNCLASSIFIED 080043-1-M F/G 20/1 NL

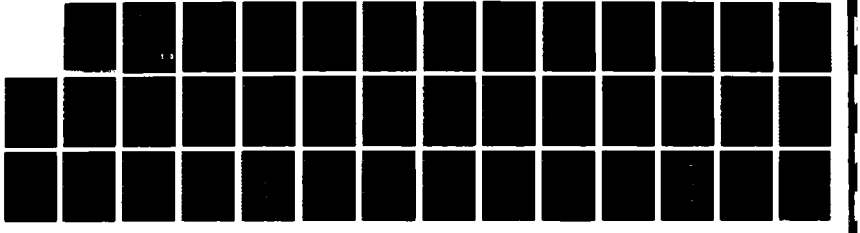

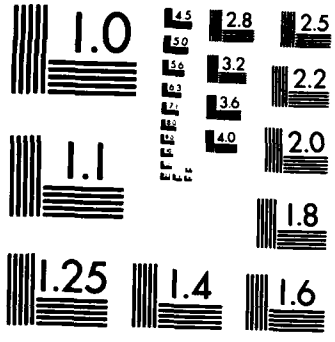

MICROCOPY RESOLUTION TEST CHART
NATIONAL BUREAU OF STANDARDS-1963-A

Report 080043-1-M

SPATIAL MATCHED PROCESSING FOR MULTIPATH PROPAGATION

M. A. Dzieciuch and T. G. Birdsall

COMMUNICATIONS & SIGNAL PROCESSING LABORATORY
Department of Electrical Engineering and Computer Science
The University of Michigan
Ann Arbor, MI 48109

November 1987

Technical Memorandum No. 121
Approved for public release; distribution unlimited.

Prepared for
OFFICE OF NAVAL RESEARCH
Department of the Navy
Arlington, Virginia 22217

UNCLASSIFIED

SECURITY CLASSIFICATION OF THIS PAGE

REPORT DOCUMENTATION PAGE

1a. REPORT SECURITY CLASSIFICATION Unclassified	1b. RESTRICTIVE MARKINGS None
2a. SECURITY CLASSIFICATION AUTHORITY	3. DISTRIBUTION/AVAILABILITY OF REPORT Approved for public release; distribution unlimited
2b. DECLASSIFICATION/DOWNGRADING SCHEDULE	
4. PERFORMING ORGANIZATION REPORT NUMBER(S) 080043-1-M TM 121	5. MONITORING ORGANIZATION REPORT NUMBER(S)
6a. NAME OF PERFORMING ORGANIZATION Communications & Signal Processing Laboratory 6b. OFFICE SYMBOL (If applicable)	7a. NAME OF MONITORING ORGANIZATION Office of Naval Research
6c. ADDRESS (City, State, and ZIP Code) The University of Michigan Ann Arbor, Michigan 48109-2122	7b. ADDRESS (City, State, and ZIP Code) 800 North Quincy Street Arlington, Virginia 22217
8a. NAME OF FUNDING/SPONSORING ORGANIZATION 8b. OFFICE SYMBOL (If applicable)	9. PROCUREMENT INSTRUMENT IDENTIFICATION NUMBER Contract No. N00014-87-K-150
8c. ADDRESS (City, State, and ZIP Code)	10. SOURCE OF FUNDING NUMBERS PROGRAM ELEMENT NO. / PROJECT NO. / TASK NO. / WORK UNIT ACCESSION NO.

11. TITLE (Include Security Classification)

SPATIAL MATCHED PROCESSING FOR MULTIPATH PROPAGATION

12. PERSONAL AUTHOR(S)
M. A. Dzieciuch and T. G. Birdsall

13a. TYPE OF REPORT	13b. TIME COVERED	14. DATE OF REPORT (Year, Month, Day)	15. PAGE COUNT
Tech. Memorandum	FROM _____ TO _____	November 1987	36

16. SUPPLEMENTARY NOTATION

17. COSATI CODES			18. SUBJECT TERMS (Continue on reverse if necessary and identify by block number)
FIELD	GROUP	SUB-GROUP	Signal Processing Underwater Acoustic Propagation Channel Matched Filtering

19. ABSTRACT (Continue on reverse if necessary and identify by block number)

Underwater acoustic propagation is characterized by multipath or multimode propagation. Ray theory and mode theory are not fully adequate for modeling physical reality. Impulse responses can be more accurately calculated using Gaussian beam theory. Signal processors can be designed to take advantage of the channel complexity if the propagation is actually known so that detectability is increased. The proposed technique, channel matched filtering, synthetically backpropagates the wave front to a hypothesized source location. Accurate passive estimates can be made without knowledge of signal characteristics. GB theory can easily accommodate a range-dependent deep water environment.

20. DISTRIBUTION/AVAILABILITY OF ABSTRACT ☒ UNCLASSIFIED/UNLIMITED ☐ SAME AS RPT. ☐ DTIC USERS	21. ABSTRACT SECURITY CLASSIFICATION Unclassified
22a. NAME OF RESPONSIBLE INDIVIDUAL Carol S. Van Aken	22b. TELEPHONE (Include Area Code) 313-764-5220 / 22c. OFFICE SYMBOL

DD FORM 1473, 84 MAR 83 APR edition may be used until exhausted. All other editions are obsolete.

SECURITY CLASSIFICATION OF THIS PAGE
UNCLASSIFIED

Spatial Matched Processing for Multipath Propagation

Matthew Dzieciuch and T. G. Birdsall
Communications and Signal Processing Laboratory
Department of Electrical Engineering and Computer Science
The University of Michigan

November 16, 1987

Abstract

Underwater acoustic propagation is characterized by multipath or multimode propagation. Ray theory and mode theory are not fully adequate for modeling physical reality. Impulse responses can be more accurately calculated using Gaussian beam theory. Signal processors can be designed to take advantage of the channel complexity if the propagation is actually known so that detectability is increased. The proposed technique, channel matched filtering, synthetically backpropagates the wave front to a hypothesized source location. Accurate passive estimates can be made without knowledge of signal characteristics. GB theory can easily accommodate a range-dependent deep water environment.

Introduction

Underwater acoustics has always been hampered by a complicated multipath environment. It can be demonstrated however, that the complex arrival structure can actually be used to the signal processor's advantage. The essential element is, of course, good modeling of ocean acoustic properties. The study of techniques which utilize precise knowledge of the acoustic propagation is the proposed thesis problem.

It is well known that low frequency sound ($\sim$ less than 1KHz) can travel several megameters underwater without prohibative attenuation (Ref. 12). The transmission of energy over such great distances is facilitated by two facts. The first is that sound is attenuated about 25dB per Mm per $(\text{kHz})^2$ at low frequencies. This means that the medium does not absorb too much of the sound energy. The second is that the sound speed profile (fig. 1) has a minimum at a depth of approximately one kilometer. This means that the energy is ducted as in a waveguide and that boundary losses are not incurred for purely refracted rays.

Another well documented characteristic of the ocean acoustic channel is multipath propagation (Ref. 6). A typical impulse response is shown in figure 2. More insight into the physics of propagation can be obtained by considering the timefront of an impulse. Timefronts are the locus of endpoints of rays which have travelled an equal amount of time from the source. Figures 3–5 show the evolution of a timefront. As the sound propagates further and further, the timefront folds accordion–like generating new sheets. The sheets of the timefront correspond to the different arrivals that are apparent in the impulse response.

In order to deal with the multipath propagation problem a new signal processor is proposed which synthetically back-propagates the wavefront to a hypothesized source location. This technique is analagous to phase conjugation methods popular in optics. It is similar to the matched field processing first described by Bucker (Ref. 1) and more recently by Clay (Ref. 3). Wax and Kailath have considered localization, but not in the multipath ocean environment. The motivation for the

back-propagation method is to refocus the signal energy, which is dispersed both in time and space, to a particular source location. By concentrating the energy, signal detectability should increase. By searching over a set of hypothesized source locations, a source position estimate can be made.

Ocean Acoustic Modeling

Good modeling of ocean acoustic propagation is essential to good signal processing. Efficiency or ease of calculation is just as important as model accuracy and consistency. There are two main schools of thought in acoustic modeling. They are known as ray theory and mode theory. Neither of these is totally acceptable for our purposes. We shall consider their shortcomings and suggest gaussian beam theory as an improvement on ray theory. In order to simplify this discussion, we shall consider only two–dimensional models here.

All models attempt to provide a solution to the wave equation.

$$\frac{\partial^2 u}{\partial x^2} + \frac{\partial^2 u}{\partial z^2} = \frac{1}{c^2}\frac{\partial^2 u}{\partial t^2}$$

In this formulation, x is the range coordinate, z is the depth coordinate, $c = c(x, z)$ denotes the sound speed, and t is time. The quantity $u(x, z, t)$ may represent various physical quantities, such as the pressure or density.

In the ray theory view of the world, one assumes a solution to the wave equation of the form:

$$u(x, z, t) = A(x, z)\exp^{j\omega[t - T(x,z)]}$$

Now inserting the solution into the wave equation and taking the limit as ω goes to infinity, one gets the eikonal equation.

$$\left(\frac{\partial T}{\partial x}\right)^2 + \left(\frac{\partial T}{\partial z}\right)^2 = \frac{1}{c^2}$$

The locus of points where T is constant defines an *isotemporal surface*, or *timefront.*

In order to model a point source with ray theory one traces a number of rays from the source, over an angular distribution, to the receiver. The amplitude response is then inversely proportional to the spacing of adjacent rays at the receiver. For an accurate estimate of arrival time, one must compute the travel time of an eigenray, the ray that goes through the receiver location.

Tracing rays on a digital computer is a fairly easy thing to do. This accounts for the popularity of ray theory. The arrival time estimates are very accurate and it is easy to include a range dependent sound speed profile. The main disadvantage with ray theory is that the amplitude estimate is not always accurate. The theory predicts infinite amplitude at caustics, which are where neighboring raypaths cross. It predicts zero amplitude in shadow zones. These do not match physical reality. Another problem is that in order to get accurate time of arrival estimates one must trace eigenrays. Practically speaking this means that many rays with different initial conditions must be traced until a ray that goes through (or comes close to) the receiver location is found.

Mode theory solutions to the wave equation overcome some of the inadequacies of ray theory. The cost is complexity of calculation and a very small collection of boundary geometries that admit solutions. The solution entails the calculation of eigenfunctions which are frequency dependent. A necessary assumption is that the sound speed is range independent. This means that the eigenfunctions vary with depth only. One approach to the solution is to match the boundary conditions at the surface and then iterate the eigenvalue until the boundary conditions at the bottom are satisfied. Given the correct eigenfunctions, the amplitude response of the channel can be accurately calculated anywhere in the channel. So for a broadband signal the eigenfunctions must be calculated across the spectrum. With all these difficulties, it is not hard to understand why ray theory is popular.

There is an alternative. Gaussian beam theory offers the best of both theories. It allows easy calculation of the channel impulse response and accurate amplitude estimates. Also it can use a range dependent sound speed profile and it does not require eigenray tracing for accurate time of arrival estimates.

It is well known that the high frequency wave field propagates mostly along rays. Gaussian beam theory seeks solutions to the wave equation which are concentrated close to each selected ray Ω. Define an orthogonal coordinate system (s, n) along

the ray. The coordinate s measures the arclength along the ray from an arbitrary reference point, n represents a length coordinate in the direction perpendicular to Ω at s. Rewrite the wave equation in the new coordinate system. The *parabolic approximation* to the wave equation is used to obtain solutions close to the ray. A complete derivation is given by Červený (Ref. 2). The solution which has the form

$$u(s,n,t) = \Psi \left[\frac{c(s)}{q(s)}\right]^{1/2} \exp\left[-j\omega\left(t - \int_{s_0}^{s} \frac{ds}{c(s)}\right) + \frac{i\omega}{2}\frac{p(s)}{q(s)}n^2\right]$$

can then be found.

The central axis of the beam obeys the standard ray trace equations. For the two dimensional case a system of four first order linear differential equations describes the raypaths.

$$\frac{dx}{dt} = c^2 A$$
$$\frac{dA}{dt} = -\frac{1}{c}\frac{dc}{dx}$$
$$\frac{dz}{dt} = c^2 B$$
$$\frac{dB}{dt} = -\frac{1}{c}\frac{dc}{dz}$$

A and B are dummy variables. The initial conditions are related to the source location and the initial angle that the ray has when it leaves the source. The values of p and q along the ray can then be found as the solution to two additional first order linear differential equations subject to some initial conditions.

$$\frac{dp}{ds} = -\frac{c_{nn}}{c^2(s)}q(s)$$

$$\frac{dq}{ds} = c(s)p(s)$$

Where c_{nn} denotes the second partial derivative of the sound speed with respect to the normal coordinate. Both p and q are complex quantities and do not depend on frequency. The solution can be rewritten as

$$u(s,n,t) = \Psi \left[\frac{c(s)}{q(s)}\right]^{1/2} \exp\left[-j\omega\left[t - \tau(s)\right] + \frac{i\omega}{2c}K(s)n^2 + \frac{n^2}{L^2(s)}\right]$$

where

$$K(s) = c(s)\, Re\left(\frac{p(s)}{q(s)}\right)$$

$$L(s) = \left[\frac{\omega}{2} Im\left(\frac{p(s)}{q(s)}\right)\right]^{-1/2}$$

$$\tau(s) = \int_{s_0}^{s} \frac{ds}{c(s)}$$

From the physical point of view, K denotes the curvature of the phase front of the beam, and L is a frequency dependent effective half-width of the beam.

Having solved the parabolic wave equation near a single beam, if we want to model a source we must fit a set of Gaussian beams to the initial wave field. The wave field $u(M)$ at the point M can be expressed in terms of Gaussian beams as

$$u(M) = \sum_{\phi} \Phi(\phi)\, u_{\phi}(s, n)$$

where ϕ is the index connected with ray Ω, and the arbitrary function $\Phi(\phi)$ is specified by the initial source field.

Once the wave field due to a source at point $\mathcal{S}$ and a receiver at any point $\mathcal{R}$ in the ocean acoustic channel is known, the impulse response from $\mathcal{S}$ to $\mathcal{R}$ can be written.

$$h(t) = \sum_{i=1}^{N} \mathcal{A}_i \delta(t - \tau_i)$$

The advantage of Gaussian beam theory is that for only slightly more computational effort than for conventional ray theory, accurate values for the $\mathcal{A}_i$'s can be calculated. It should be pointed out that although p and q are independent of frequency, $\mathcal{A}_i$ and τ_i are theoretically weakly dependent on frequency. Our best information is that in the real ocean $\mathcal{A}_i$ and τ_i do not change appreciably over the range of frequencies (5–500 Hz) that we are interested in (Ref. 5). The question of sensitivity of the impulse response to frequency needs to be studied further.

All the models considered so far are deterministic. Ocean variability is a very complex phenomena but its main component is thought to be internal waves. Experimentally it has been shown that it is the amplitude of the arrivals that varies

the most. Amplitude stability is on the order of ten minutes. Time of arrival is actually quite stable, variations less than milliseconds over periods of days (Ref. 6). Even crude simulations of internal wave effects confirm this behavior. Investigation of amplitude variance vis–à–vis travel time variance would be reasonable and interesting. It has been hypothesized that $\partial^2 c/\partial z^2$ affects the former strongly and the latter weakly.

Signal Processing

Taking a systems approach, we want to apply statistical communications theory and signal detection and estimation theory to the ocean acoustic situation. It is crucial to realize that this is a multiple source and multiple sensor environment and that sources and sensors are coupled by more than one path.

The question we wish to answer is this: If we knew $c(x, y, z, t)$, the speed of sound everywhere, what good would it do? Would we be able to use the knowledge of the acoustic transfer function to improve communications, detection, or localization?

We choose to focus on signal detectability first and we do not wish to make any assumptions about the nature of the source signals. Before proposing any new detection algorithms one has to ask why is the standard theory of signal detectability inadequate. The likelihood ratio theory of signal detectability is essentially a hypothesis testing theory (Ref. 1, 13). The most general problem might be set up by considering a distribution of source locations in three dimensional space. Given a specific realization $\mathcal{R}$ of M source locations, one specifies a composite distribution for each source waveform. There is a conditional likelihood ratio $\ell(\textit{observation} \mid \mathcal{R})$ with respect to some measure. The posterior probability of a particular source distribution would entail an expectation over all $\mathcal{R}$.

Detection theory does give some guidelines. It suggests highly parallel processing of the observation, one branch for each hypothesis (perhaps each acoustic source). This in turn suggests that *linear* preprocessing be considered just prior to the inevitable non-linear processing that precedes expectations over signal parameters and final decisions.

Detection theory uses a *forward* propagating approach: it hypothesizes the causes (source positions and waveforms) and calculates how likely each would be to have caused the observed waveform. Given the muliplicity of source locations, sensor positions, and paths, this appears to be a monumental task. Therefore a direct *global* attack such as this will not be undertaken and alternatives should be sought

that do not need to hypothesize the waveforms of sources.

As shown in the last section, the ocean acoustic channel can be modeled as linear time-invariant filter of the form

$$h^U(\tau) = \sum_{p=1}^{P} \mathcal{A}_p \delta(\tau - \tau_p)$$

where U represents the position of the hydrophone relative to the source. We will use this deterministic model and ignore any variability of the ocean since it is our objective to develop new signal processing strategies based on a known acoustic transfer function.

The new processing strategy we propose to study is the *reverse* propagation of signal waveform through a linear filter which approximates the ocean channel. Suppose we wish to find the source waveform from the waveform observed at the hydrophone. We will assume that the observation, $r(t) = s(t) * h^U(t)$, is noiseless for the time being. The reverse propagating filter has the form

$$b^V(\tau) = \sum_{q=1}^{Q} \mathcal{B}_q \delta(\tau + \tau_q)$$

where V is the hypothesized position of the source relative to the hydrophone, and the $\mathcal{B}_q$'s and τ_q's are related to the forward coefficients and time delays respectively. After the filter, the output is

$$w(t) \triangleq r(t) * b^V(t) = \sum_{p=1}^{P} \sum_{q=1}^{Q} \mathcal{A}_p \mathcal{B}_q s(t - \tau_p + \tau_q)$$

Now if the reverse propagating filter has correctly hypothesized the source position, $w(t)$ becomes

$$w(t) = \sum_{p=1}^{P} \mathcal{A}_p \mathcal{B}_p s(t) + \sum_{p=1}^{P} \sum_{q \neq p}^{P} \mathcal{A}_p \mathcal{B}_q s(t - \tau_p + \tau_q)$$

The first term has the property we want of reconstructing the original unknown source waveform. The second term is a self-interference term.

Let us now examine how we might choose the coefficients, $\mathcal{B}_q$, of the reverse propagating filter. Three choices come to mind.

$$\mathcal{B}_q = \mathcal{A}_q^z$$

where $z = 1, 0,$ or -1. These correspond to a *channel matched*, a *channel phase*, and a *channel inverse* filter respectively. As z varies between 1 and -1, we might expect that we could trade signal–to–noise(or interference) ratio for *sharpness* of response. If one knew the signal and noise power spectral density at the hydrophone, the matched filter for the received waveform would be

$$\frac{S^*(\omega)H^*(\omega)}{|N(\omega)|^2}$$

The *channel matched* filter is nothing but the channel half of the matched filter. The *channel phase* and *channel inverse* filters have a less clear relationship to the standard phase only and inverse filters.

Next, let us assume that we have an array of hydrophones. Each hydrophone reception is back–propagated to a hypothesized source location and then the filter outputs are summed to get

$$a(\tau; U, V) \triangleq \sum_{p=1}^{P}\sum_{q=1}^{Q}\sum_{r=1}^{R} \mathcal{A}_{p,r}(U)\mathcal{B}_{q,r}(V)\delta(\tau - \tau_{p,r}(U) + \tau_{q,r}(V))$$

where r is the hydrophone index and R is the number of hydrophones. The function $a(\tau; U, V)$ is a psuedo-ambiguity function. It can be expected to peak when $U = V$, but the volume enclosed by it is not constant as V varies.

Let us assume that we are using channel matched filtering. There are two cases which can occur. First suppose that the back–propagating filter exactly compensates for the channel. Then we have

$$a(t; U, V) = \sum_{p=1}^{P}\sum_{r=1}^{R} \mathcal{A}_{p,r}(U)\mathcal{A}_{p,r}(U)s(t) + \sum_{p=1}^{P}\sum_{q\neq p}^{Q}\sum_{r=1}^{R} \mathcal{A}_{p,r}(U)\mathcal{A}_{q,r}(U)s(t-\tau_{p,r}(U)+\tau_{q,r}(U))$$

The first term reconstructs the original signal and the second is a self–interference term. The hope is that as R and P increase, the gain applied to the reconstruction

increases faster than that of the interfering term. This depends upon the unknown power spectral density of the source signal. Now suppose that the back-propagating filter incorrectly hypothesizes the source position. Then we have

$$a(t;U,V) = \sum_{p=1}^{P}\sum_{q=1}^{Q}\sum_{r=1}^{R} \mathcal{A}_{p,r}(U)\mathcal{A}_{q,r}(V)s(t - \tau_{p,r}(U) + \tau_{q,r}(V))$$

In this case we have only the self-interference term. Adding many signal waveforms in this incoherent fashion, we hope that the power in $a(t;U,V)$ is less than in $a(t;U,U)$ where the waveforms are added coherently.

It may be useful to perform a normalization

$$\tilde{a}(t;U,V) = \frac{a(t;U,V)}{\sqrt{\sum_{q=1}^{Q}\sum_{r=1}^{R}|\mathcal{B}_{q,r}(V)|^2 \sum_{q=1}^{Q}\sum_{r=1}^{R}|r(t+\tau_{q,r}(V))|^2}}$$

This assures that $|\tilde{a}| \leq 1$ by an application of the Schwarz inequality. Further processing of the pseudo-ambiguity function would probably resemble standard detection theory. For example the integral

$$|A(U,V)|^2 \triangleq \int_0^T \tilde{a}^2(t;U,V)\,dt$$

could be formed and an energy detector would then be realized.

The ability of an array of back-propagating filters to localize a source depends on the complexity of the arrival structure. Generally speaking the more complicated the structure the easier it becomes to localize a source. This happens because of the fact that more structure is equivalent to more information about the channel. Thus we have used the multipath channel characteristic to our advantage.

The total array signal gain is the ratio of the power in the reconstructed signal term to the power of the signal in the largest path. The power in the reconstructed signal term is proportional to PR, the number of hydrophones R, and the number of paths P. One cannot say what the reconstruced signal power will be in general without specifing where the source is because the answer depends on the path coefficients $\mathcal{A}_{p,r}$. The reason for choosing the power in the largest path for the denominator instead of the power in all paths is this: In conventional signal processing

one cannot recombine paths and therefore one views the other paths as contributing interference.

The noise performance of our system is a hard thing to estimate. This is because the noise characteristics of the ocean are not known well. So much of what is normally refered to as noise is actually interference from other sources such as shipping traffic, active sonars, and drilling rigs. If it is possible to map all the major sound sources in the ocean then much of this interference could be eliminated and the ultimate ocean noise limit could be found.

Results

Results to date have been very encouraging, both in terms of modeling and in terms of signal processing.

Impulse responses have been calculated on a computer using Gaussian beam theory. This is new work and we do not believe anyone else has calculated point-to-point transfer functions using this theory. Although it has not been verified by comparison with wave theory, the responses exhibit the correct behavior at caustics and in shadow zones. An example impulse response between two points on the SOFAR axis is given in figure 2. This was calculated using a Munk canonical sound speed profile and the two points are 500 kilometers apart.

The pseudoambiguity function has been calculated in a number of test cases and it exhibits the correct response. The response peaks at the true source location and decreases as the hypothesized source position moves away from the true position. In figure 6, the maximum over time of the unnormalized matched pseudoambiguity function is plotted versus range.

$$\max_{\tau} a(\tau; U, V) = \max_{\tau} \sum_{p=1}^{P} \sum_{q=1}^{Q} \sum_{r=1}^{R} \mathcal{A}_{p,r}(U) \mathcal{A}_{q,r}(V) \delta(\tau - \tau_{p,r}(U) + \tau_{q,r}(V))$$

The true source location is at 250 kilometers, where the peak is. The search depth was held fixed at the true search depth. Channel matched filtering works.

For the next several cases we will consider a slightly different function. Suppose the source waveform is known to be a sinusoid. Then the pseudoambiguity function becomes

$$a(t; U, V) = \sum_{p=1}^{P} \sum_{q=1}^{Q} \sum_{r=1}^{R} \mathcal{A}_{p,r}(U) \mathcal{B}_{q,r}(V) \cos[\omega(t - \tau_{p,r}(U) + \tau_{q,r}(V))]$$

We will evaluate this function at $t = 0$ for a variety of cases.

Consider first the ***phase only*** filter. The response is plotted versus search range for a source at 500 Hz in figures 7–9. The function becomes better behaved as the true range is increased and the number of hydrophones in the array is increased.

Now we will consider the *matched* filter case. In figure 10, the source is located 100 kilometers from the array. Both source and array are at a depth of 1200 meters. The response function becomes much smoother than in the *phase* only filter case. The sidelobe structure also becomes much more defined. The magnitude of the sidelobes is a cause for worry though. It is postulated that this behavior occurs because of convergence zone focusing. In figure 11, the number of phones is increased to 500. This has the effect of reducing the size of sidelobes compared to the unnormalized main response. The true source location is moved to 250 kilometers in figure 12. This also has the effect of reducing the sidelobe response even though in this case only 50 phones are used in the array. This is to be expected because of the greater complexity of the wavefront as range increases.

Let us now examine the depth resolution of the processing. In figures 13 and 14, the source depth is 400 meters and the array depth is 1200 meters. The search depth is 400 meters in figure 13 and 1200 meters in figure 14. The response peaks at the correct location in figure 13. When the search depth is changed the absolute value of the unnormalized response is much lower. The peak at about 290 kilometers in both plots was unexpected and is so far unexplained.

Finally, the last plot, in figure 15, shows the effect of a frequency change in the pseudoambiguity function. The parameters are the same as in figure 13 except the source is now at 100 Hz.

Future Work

As seen in the last section, channel matched filtering is a viable technique. Many basic questions about the performance of back–propagating processing need to be answered however. The performance measures which we are interested in, include signal detectability, localization resolution, array gain, and noise or interference rejection. The two most critical issues are probably array geometry and location aliasing.

Array geometry is somewhat limited by physical constraints. We wish to examine the theoretical performance of different configurations without regard to hardware or computational costs however. Different configurations could include: a small densely instrumented sensor array in the horizontal; a convergence zone sized sparsely instrumented sensor array in the horizontal; a top–to–bottom stiff densely instrumented vertical array in conjunction with a conventional sparsely instrumented horizontal array.

Location aliasing is manifested in the ambiguity of which convergence zone a source may be in. This question is probably intimately related to the particular array geometry. Performance in this respect could possibly be improved by implementing a scheme similar to null steering; that is, by trying to reduce the sidelobe response where it is magnified by convergence zone focusing. A full scale, three dimensional examination of the pseudoambiguity function would be informative. The increase in dimensionality might improve localization performance since would increase the complexity of the wavefronts considered.

Another important issue is the signal characteristics. As signal bandwidth is increased the performance of the array should improve. This happens because more bandwidth would again increase the waveform complexity.

One question is what is the ultimate performance limit of matched channel processing. A useful approach may be to consider how well we could image a source if we know the wavefront exactly on some continuous smooth surface. Perhaps we

could learn what the best surface sheet geometry would be. Also it might be possible to relate resolution to aperture size.

If two or more sources are present, standard techniques in signal processing may be applied to improve performance. In order to seperate sources high resolution spectral estimation techniques may be used (Ref. 9). Also recursive methods (Ref. 10) could be employed to cancel energy from known or previously identified interferers.

An improvement may be made to the channel matched filter processing by attempting to resolve the paths. The Gaussian beam model specifies the angle of arrival of different paths. This information is ignored currently and the waveform is back-propagated in all directions. If one is able to resolve the paths (which are distibuted over about 30 degrees) then the back-propagation could be done only in the direction of the hypothesized source. This technique could vastly improve the self-interference performance.

Finding the location of a source by channel matched filtering can be looked upon as the solution of an inverse problem by forward modeling. In the usual situation we have

$$R(f) = S(f)H(f) + N(f)$$

where S(f) is the source spectrum, H(f) is the channel transfer function, and R(f) is the observed spectrum. We wish to form an estimate of some channel parameters such as the range, depth, and bearing angle. This task may be performed in two ways. The usual method is to directly perform an inversion operation on R(f)

$$\hat{H}(f) = \frac{R(f)}{S(f)}$$

to obtain the channel parameters. The problem with this method is that the inversion operation is often very sensitive. That is to say small changes in R(f) will produce large changes in the estimated channel parameters. This is directly solving the inverse problem.

There is another method of solving for the channel parameters. In this method a model for H(f) is postulated that uses the desired estimates of channel parameters as inputs. A whole class of transfer functions can then be generated. Note that this class is a subset of the class of transfer functions estimated by the direct procedure. The best estimate of the channel parameters is then found by finding the $H(f)$ which maximizes

$$\frac{R(f)S^*(f)H^*(f)}{|N(f)|^2}$$

This is the structure that is used in the proposed thesis problem and is known as solving the inverse problem by forward modeling. Formalizing this algorithm would be an interesting and useful exercise. Some work has been done in this area by Jaynes (Ref. 8).

Another consideration is the effect of Doppler shifts on the processing. When an acoustic source or receiver is moving with respect to the medium a frequency shift in the received signal is observed. Note that this shift is different for all paths. This is because all paths have different takeoff and arrival angles. The amount of doppler shift is then proportional to the dot product of the source (or receiver) velocity vector and the path takeoff (or arrival) vector.

Finally, the application of channel matched filtering to real data must be considered. How this might be done is not clear. There is much data available on long range acoustic transfer functions. The data was generated by the Ocean Acoustic Tomagraphy Group of which CSPL is a member. This data could therefore be easily accessed.

References

1. T. G. Birdsall, *The Theory of Signal Detectability: ROC Curves and Their Character*, Ph.D. Thesis, The University of Michigan, 1966.

2. Homer P. Bucker, "Use of calculated sound fields and matched-field detection to locate sound sources in shallow water", *Journal of the Acoustic Society of America*, 1976, **59**, 368–373.

3. V. Červený, M. M. Popov, and I. Pšenčík, "Computation of wave fields in inhomogeneous media — Gaussian beam approach", *Geophysical Journal of the Royal Astronomical Society*, 1982, **70**, 109–128.

4. C. S. Clay, "Optimum time domain signal transmission and source location in a waveguide", *Journal of the Acoustic Society of America*, 1987, **81**, 660–664.

5. B. Cornuelle, et. al., "Tomographic Maps of the Ocean Mesoscale. Part 1: Pure Acoustics", *Journal of Physical Oceanography*, 1985, **15**, 133–152.

6. Stanley M. Flatté, Ed., *Sound transmission through a fluctuating ocean*, Cambridge University Press, 1979.

7. S. Haykin, Ed., *Array Signal Processing*, Prentice-Hall, 1985.

8. E. T. Jaynes, "Prior Information and Ambiguity in Inverse Problems", *Proceedings of the Symposium in Applied Mathematics of the American Mathematical Society and the Society for Industrial and Applied Mathematics*, 1983, **14**, 151–166.

9. D. H. Johnson, "The Application of Spectral Estimation Methods to Bearing Estimation Problems", *Proceedings of the IEEE*, 1982, **70**, 1018–1028.

10. L. Ljung and T. Söderström, *Theory and Practice of Recursive Identification*, MIT Press, 1983.

11. R. P. Porter and A. J. Devaney, "Generalized Holography and Computational Solutions to Inverse Problems", *Journal of the Optical Society of America*, 1982, **72**, 1707–1713.

12. J. C. Stienberg and T. G. Birdsall, "Underwater sound propagation in the straights of Florida", *Journal of the Acoustic Society of America*, 1966, **39**, 301–315.

13. H. L. Van Trees, *Detection, Estimation, and Modulation Theory*, John Wiley & Sons, 1968.

14. Mati Wax and Thomas Kailath, "Optimum Localization of Multiple Sources by Passive Arrays", *IEEE Transactions on Acoustics, Speech, and Signal Processing*, 1983, **31**, 1210–1217.

15. Mati Wax and Thomas Kailath, "Decentralized Processing in Sensor Arrays", *IEEE Transactions on Acoustics, Speech, and Signal Processing*, 1985, **33**, 1123–1129.

Figures

Figure 1 is Munk's canonical sound speed profile.

$$c(z) = c_0[1 + \varepsilon(\exp^{\eta} + \eta - 1)]$$

$$\eta = 2(z - z_0)/\beta$$

This is a theoretical profile developed from first order physical reasoning, and represents an oversimplified model of real sound speeds.

Figure 2 was calculated for a range of 500 kilometers, a source depth of 1200 meters, and a receiver depth of 1200 meters. The times marked correspond to the time of propagation at the edges of the graph. The height of the impulses are proportional to the amplitude of the response.

Figures 3–5 show stages of the timefront for a source depth of 800 meters and a Munk sound speed profile. The horizontal axis is range, but magnified by 1.5 compared to vertical. Purely refracted rays with source angles between ±15 degrees are shown.

Figure 3: After 1 second the wavefront is nearly spherical.

Figure 4: After 68 seconds, two sets of wavefronts have developed. They essentially correspond to initially upward going and downward going rays.

Figure 5: After 337 seconds, the timefront is the interleave of two *accordians*, each with 8 sheets. A receiver at a depth of 1200 meters (on the axis) will have the time arrival structure shown in figure 2, with groups of 4 arrivals.

Figure 6–15 assume a horizontal line array with variable phone spacing and that the source is placed in an endfire position relative to the array. All ambiguity functions were calculated assuming a range independent Munk profile.

Figure 6: Maximum of ambiguity function with impulses sorted into 1 millisecond time bins. True source range 250,000 meters, true source depth 1200 meters, 99 phones spaced 100 meters apart at 1200 meters depth, matched processing at a search depth of 1200 meters.

Figure 7: Ambiguity function with sinusoidal source at 500 hertz, true source range 100,000 meters, true source depth 1200 meters, 100 phones spaced 100 meters apart at 1200 meters depth, phase only processing at a search depth of 1200 meters.

Figure 8: Ambiguity function with sinusoidal source at 500 hertz, true source range 250,000 meters, true source depth 1200 meters, 500 phones spaced 100 meters apart at 1200 meters depth, phase only processing at a search depth of 1200 meters.

Figure 9: Ambiguity function with sinusoidal source at 500 hertz, true source range 500,000 meters, true source depth 1200 meters, 200 phones spaced 100 meters apart at 1200 meters depth, phase only processing at a search depth of 1200 meters.

Figure 10: Ambiguity function with sinusoidal source at 500 hertz, true source range 100,000 meters, true source depth 1200 meters, 100 phones spaced 100 meters apart at 1200 meters depth, matched processing at a search depth of 1200 meters.

Figure 11: Ambiguity function with sinusoidal source at 500 hertz, true source range 100,000 meters, true source depth 1200 meters, 500 phones spaced 100 meters apart at 1200 meters depth, matched processing at a search depth of 1200 meters.

Figure 12: Ambiguity function with sinusoidal source at 500 hertz, true source range 250,000 meters, true source depth 1200 meters, 50 phones spaced 100 meters apart at 1200 meters depth, matched processing at a search depth of 1200 meters.

Figure 13: Ambiguity function with sinusoidal source at 500 hertz, true source range 250,000 meters, true source depth 400 meters, 100 phones spaced 100 meters apart at 1200 meters depth, matched processing at a search depth of 400 meters.

Figure 14: Ambiguity function with sinusoidal source at 500 hertz, true source range 250,000 meters, true source depth 400 meters, 100 phones spaced 100 meters apart at 1200 meters depth, matched processing at a search depth of 1200 meters.

Figure 15: Ambiguity function with sinusoidal source at 100 hertz, true source range 250,000 meters, true source depth 400 meters, 100 phones spaced 100 meters apart at 1200 meters depth, matched processing at a search depth of 1200 meters.

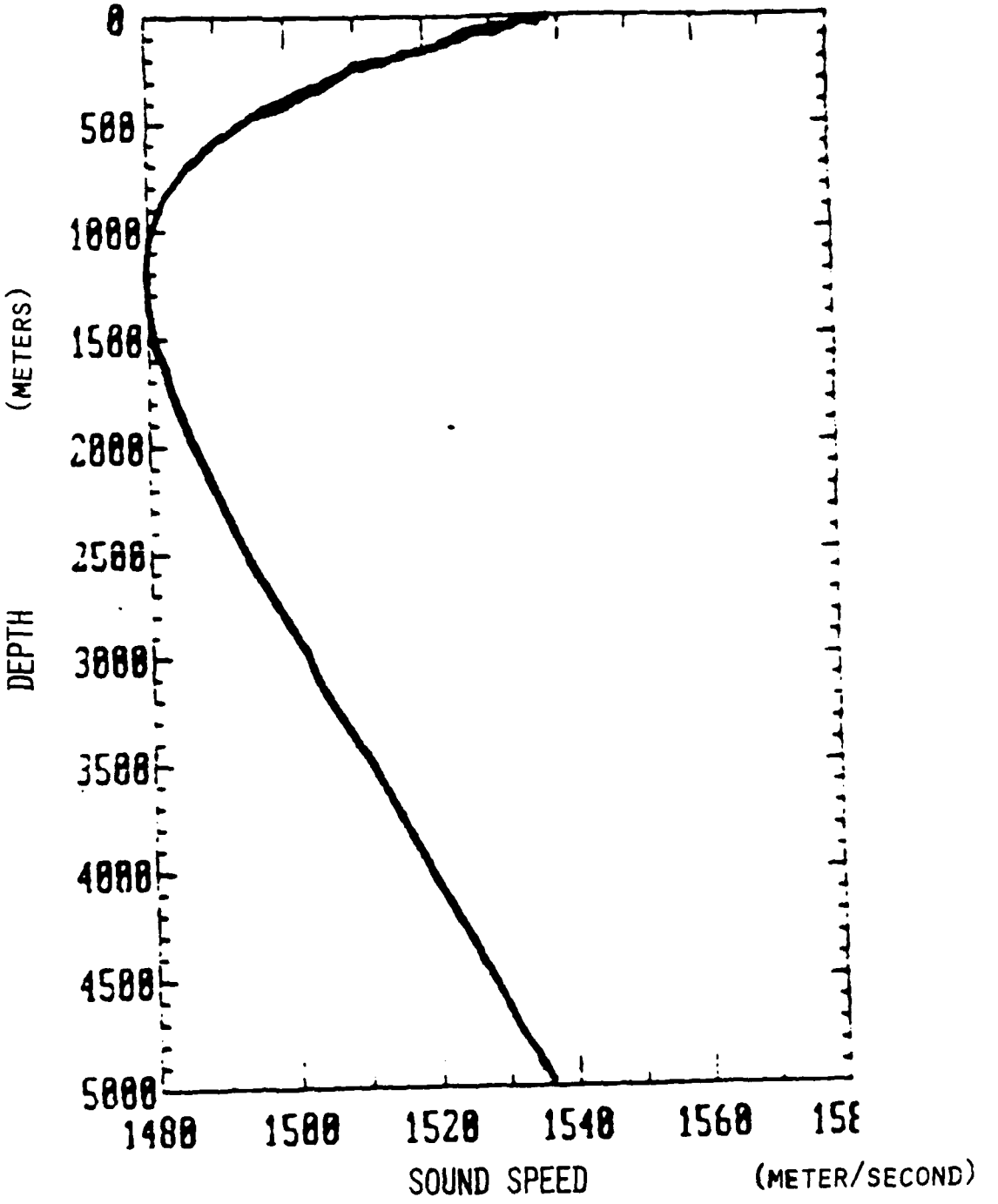
0
500
1000
1500
2000
2500
3000
3500
4000
4500
5000
DEPTH
(METERS)
1480
1500
1520
1540
1560
SOUND SPEED
(METER/SECOND)

FIGURE 1

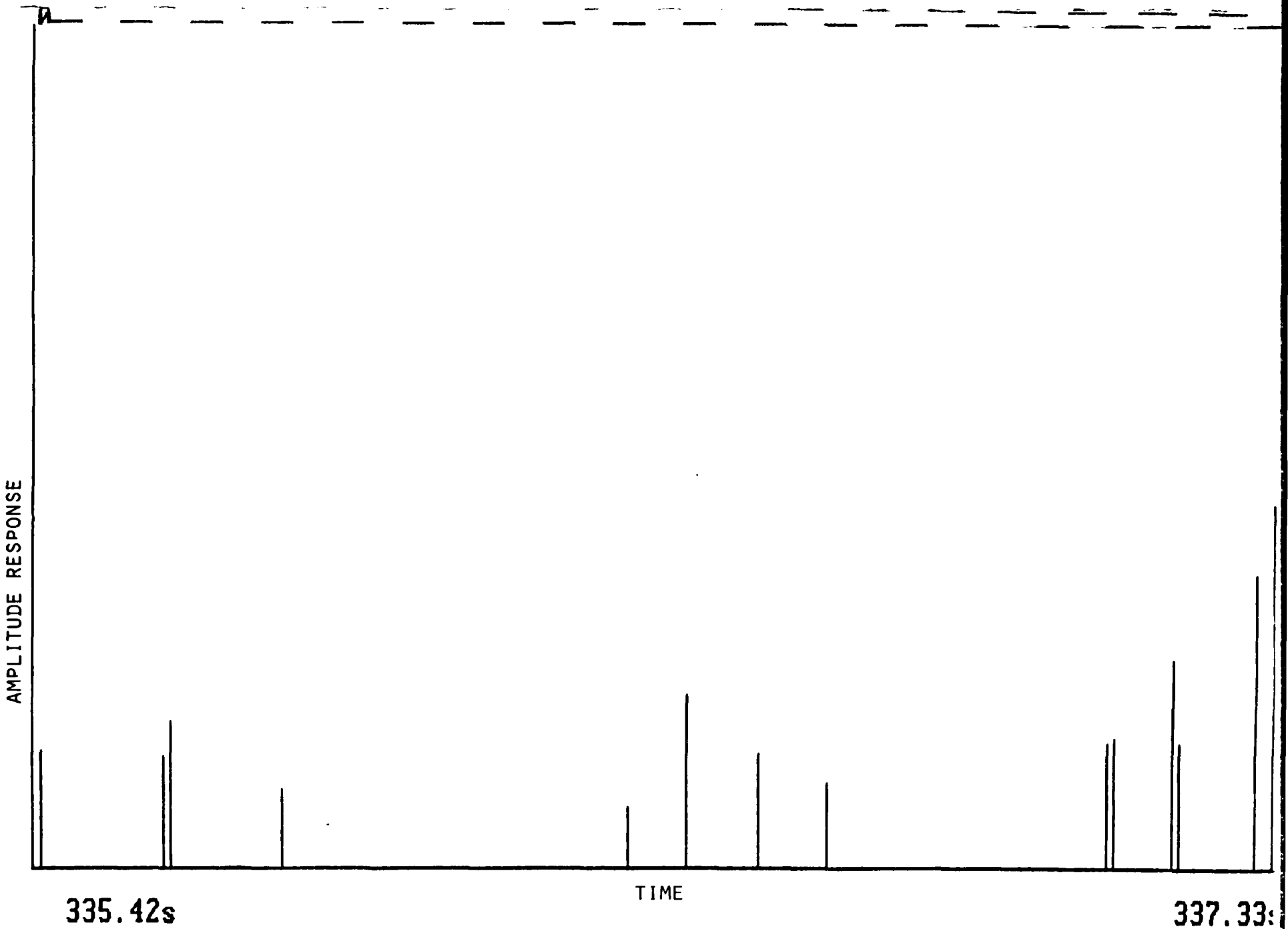

FIGURE 2. IMPULSE RESPONSE

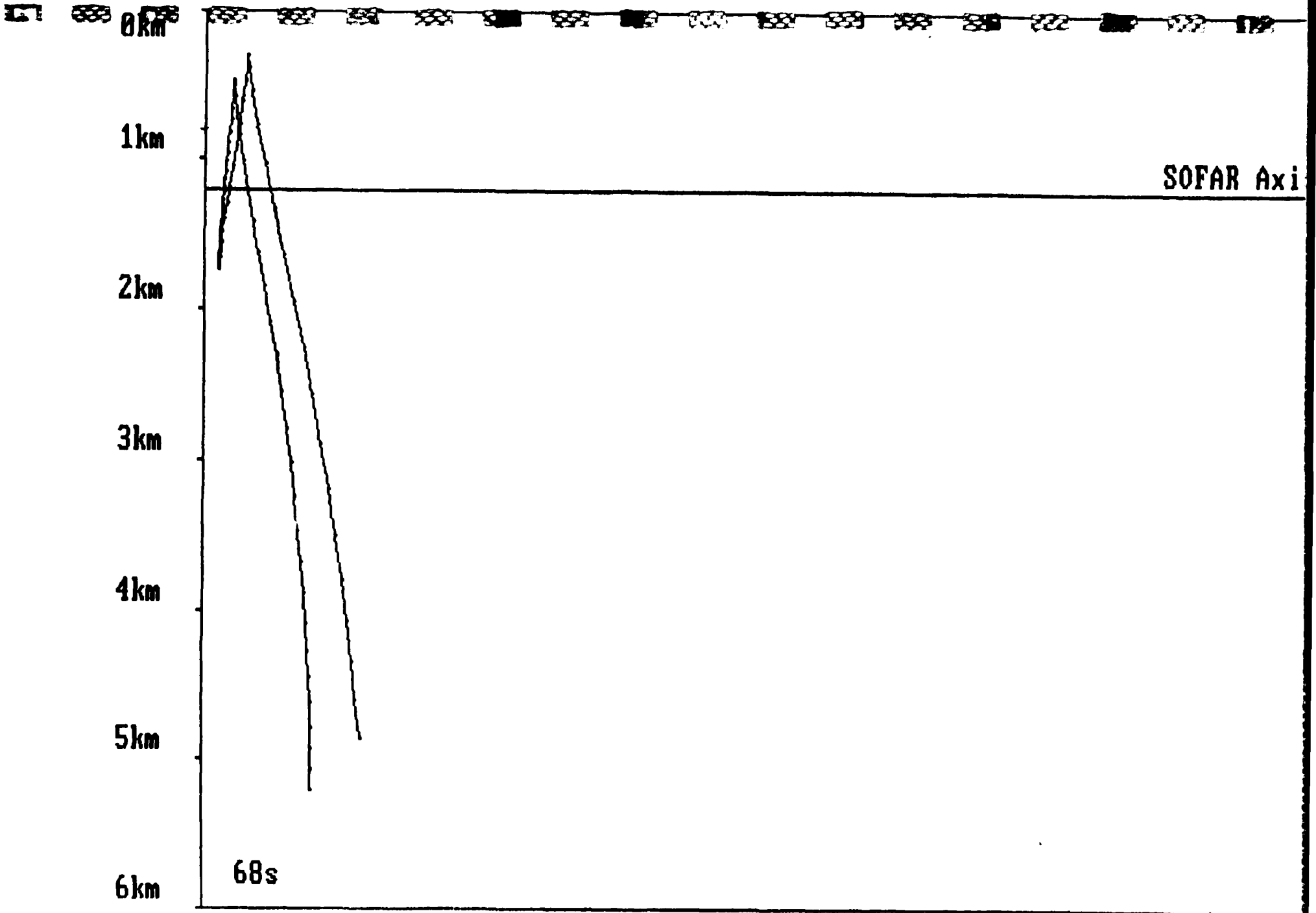

FIGURE 4

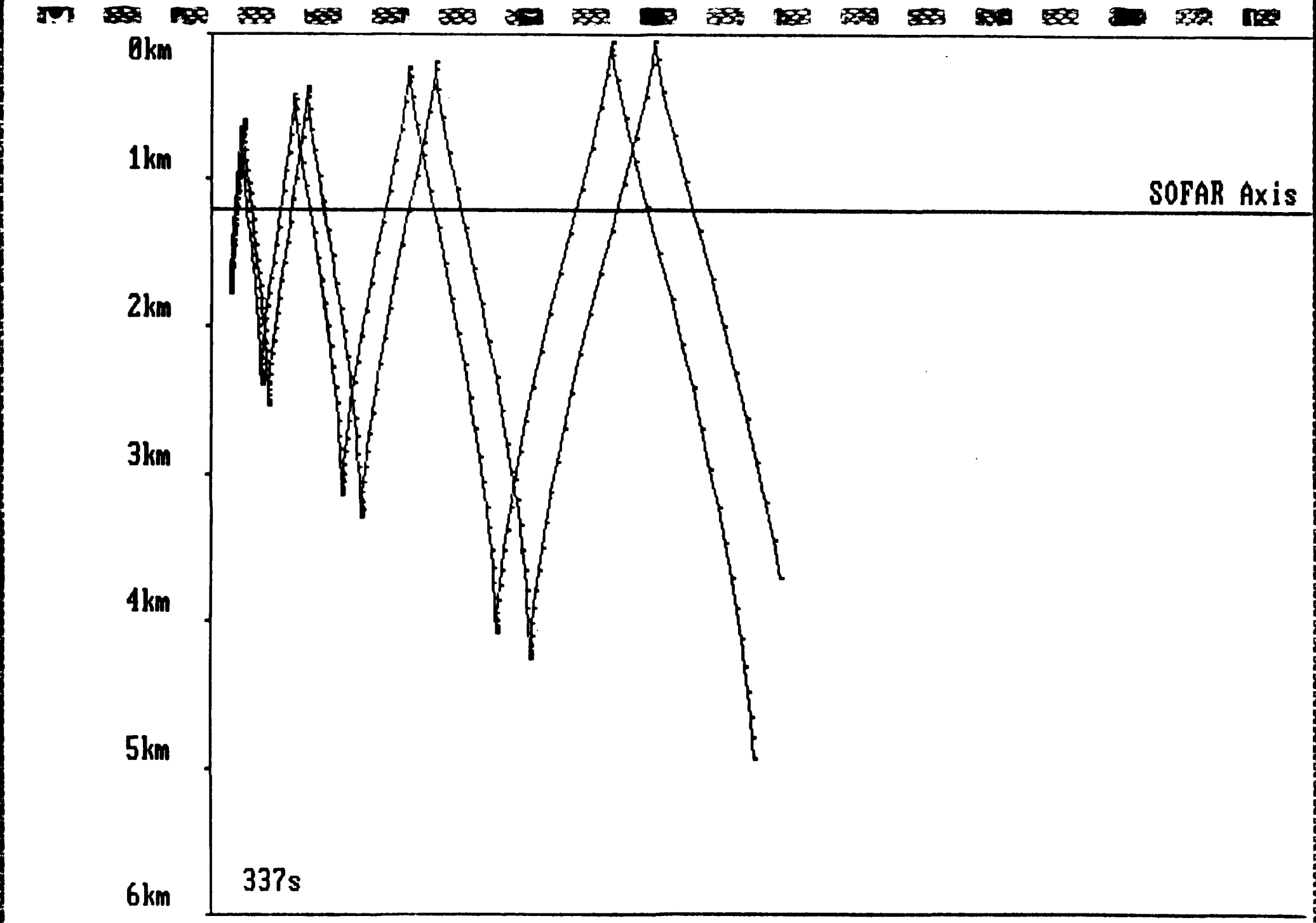

FIGURE 5

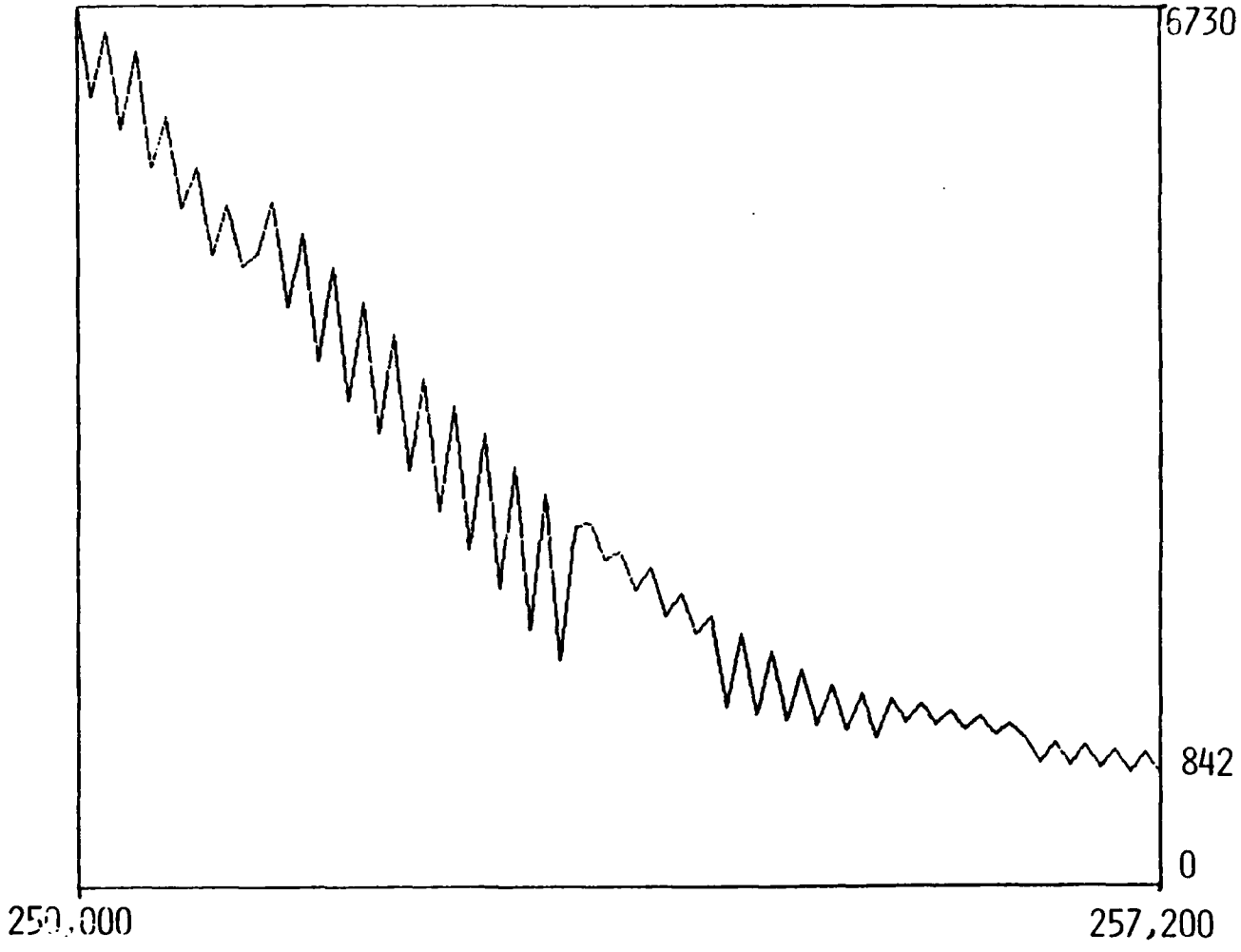

FIGURE 6

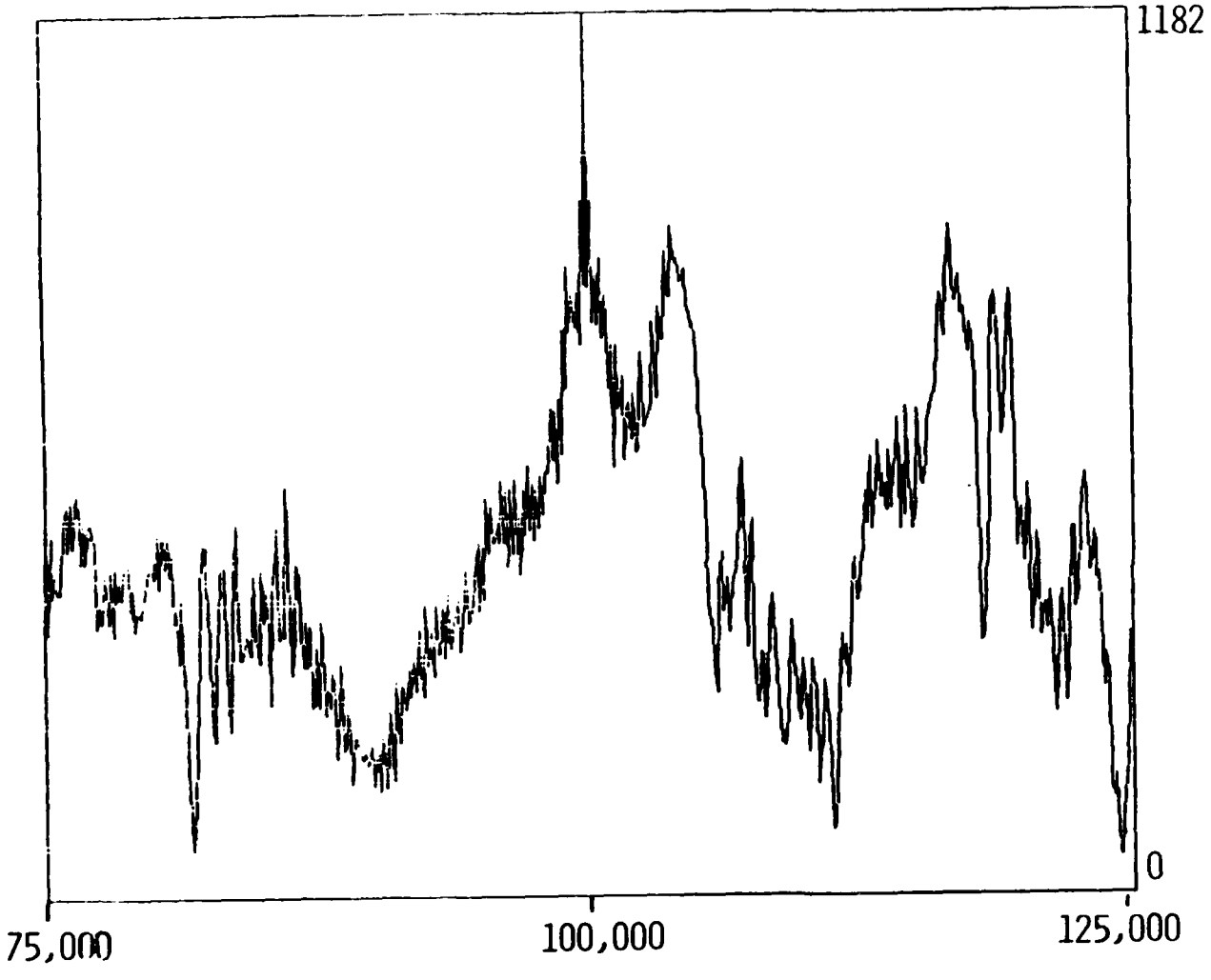

FIGURE 7

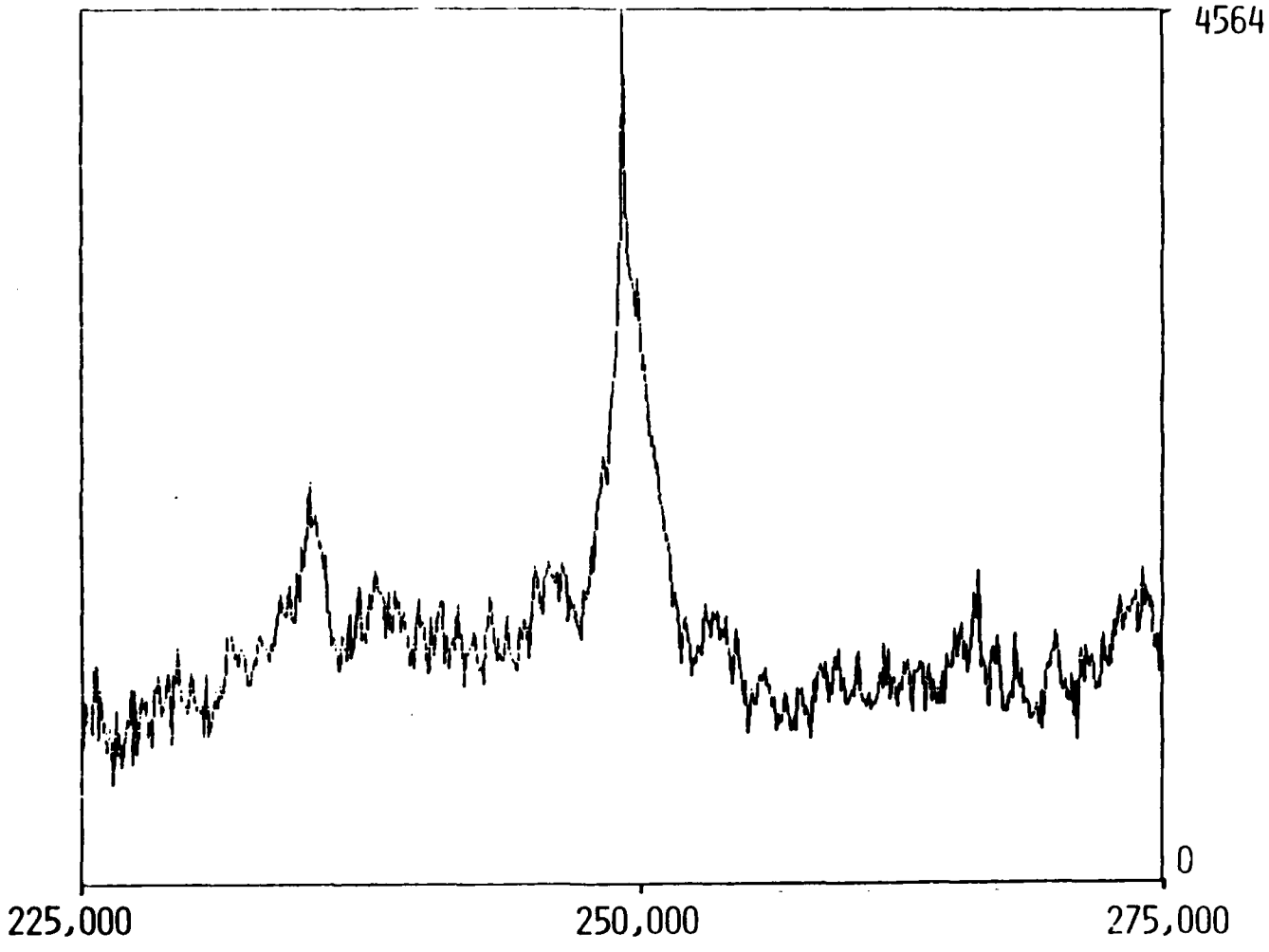

FIGURE 8

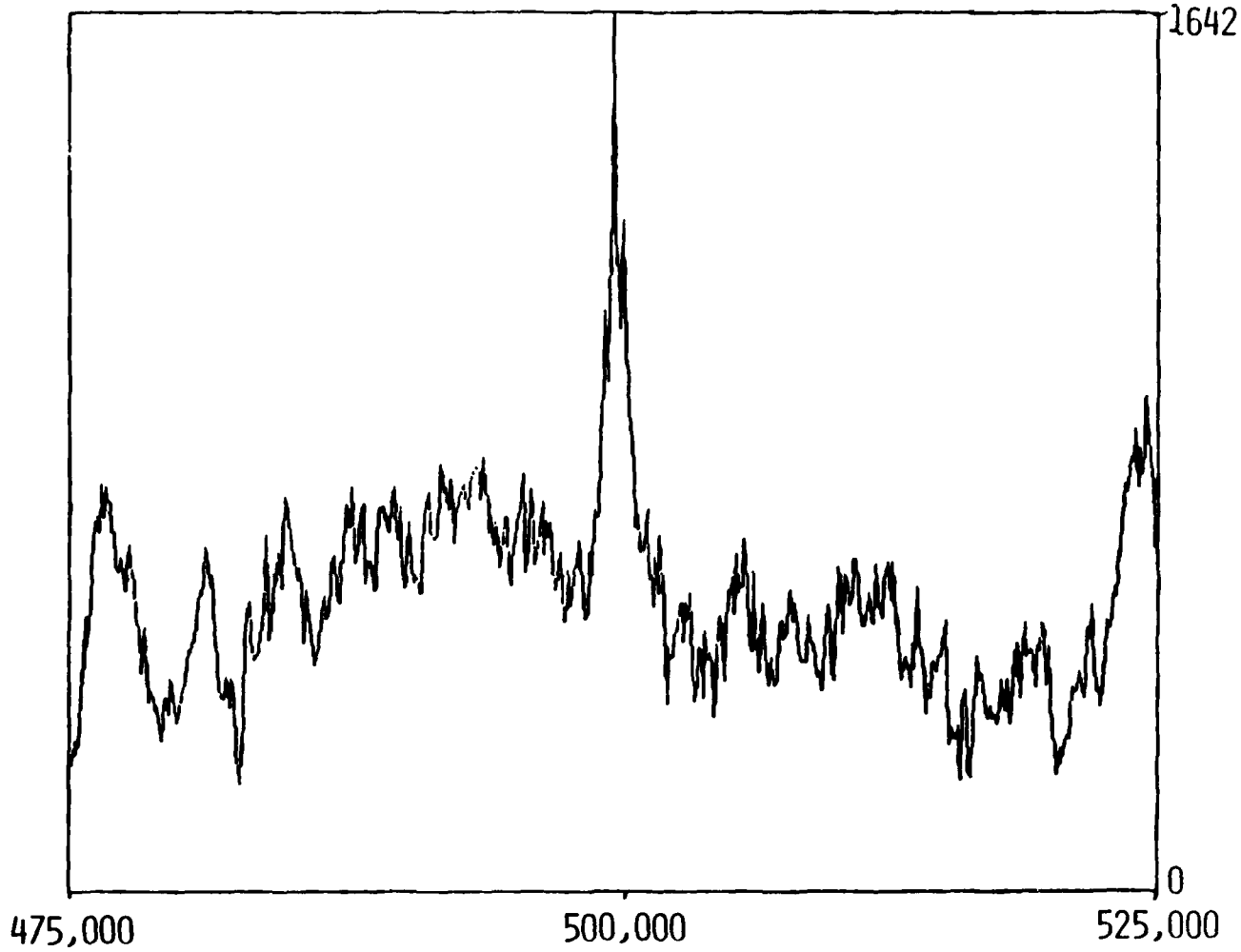

FIGURE 9

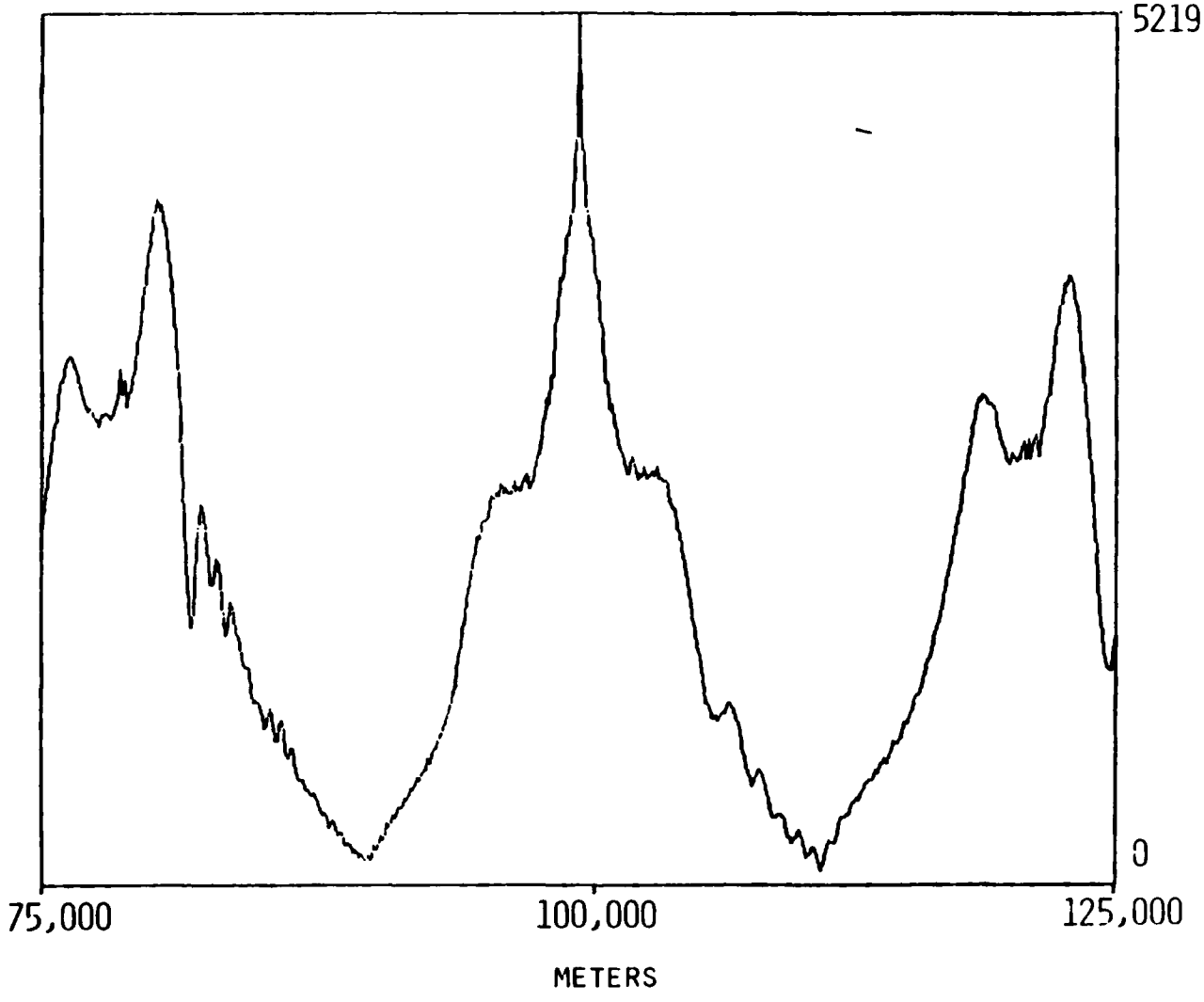

FIGURE 10

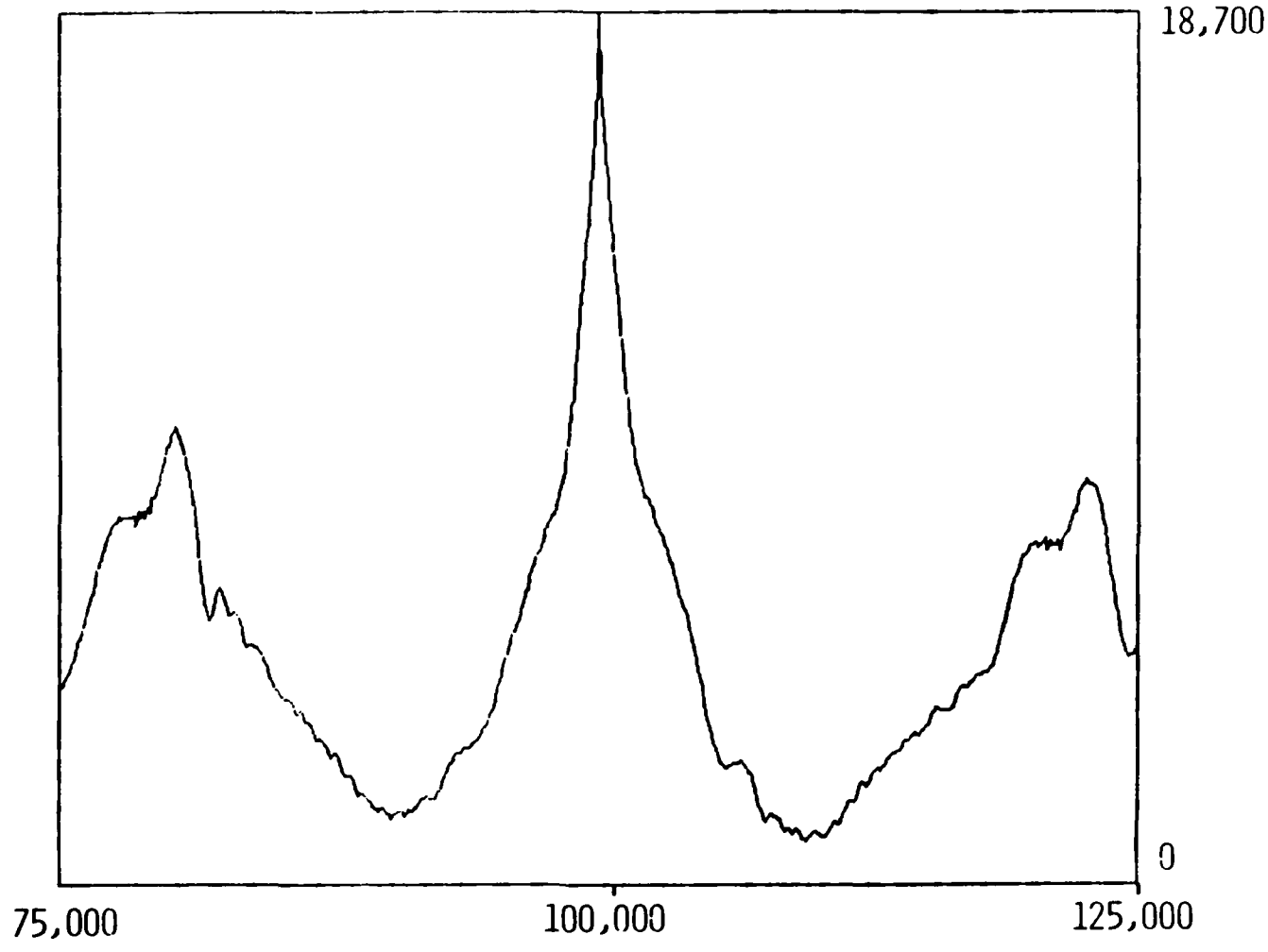

FIGURE 11

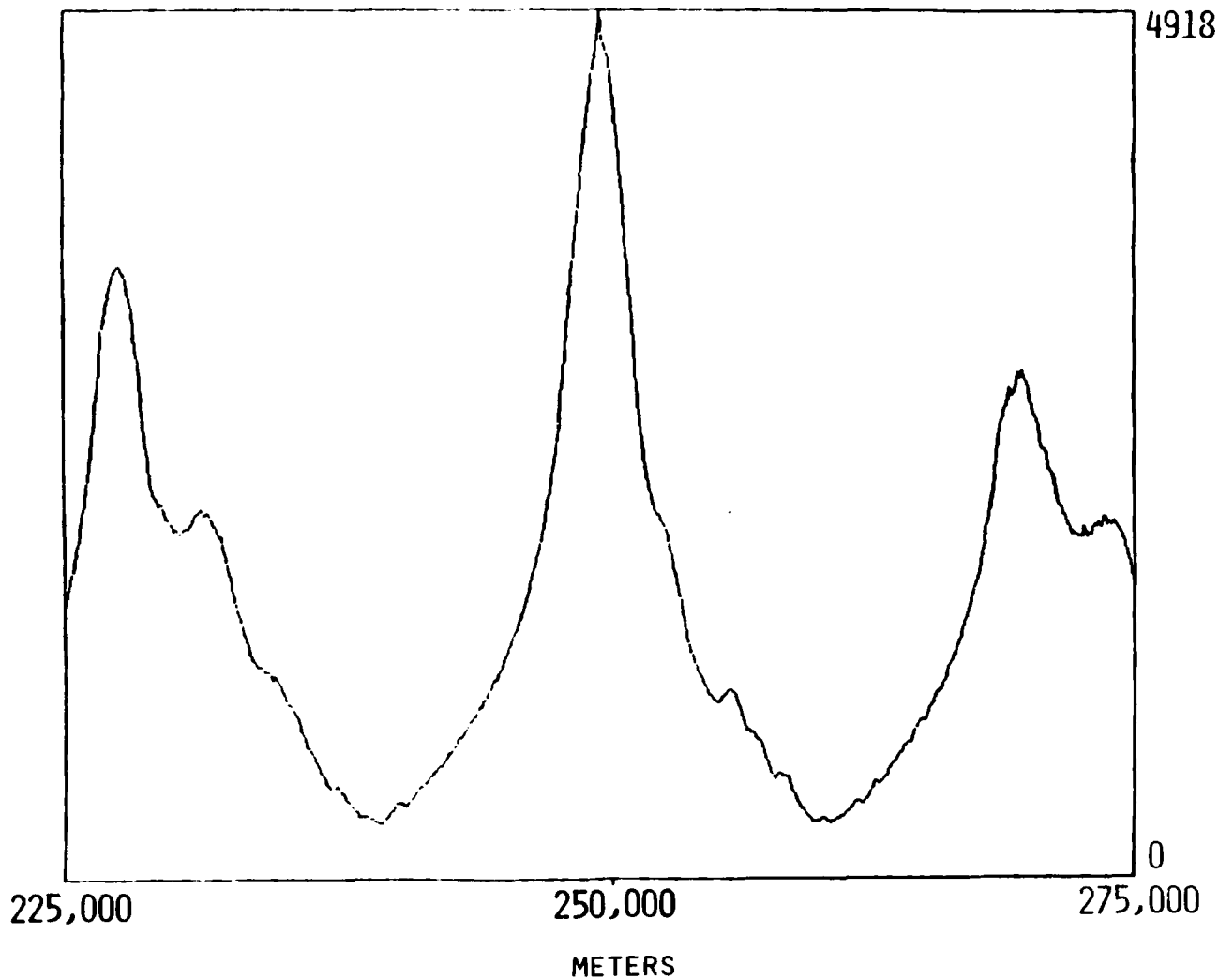

FIGURE 12

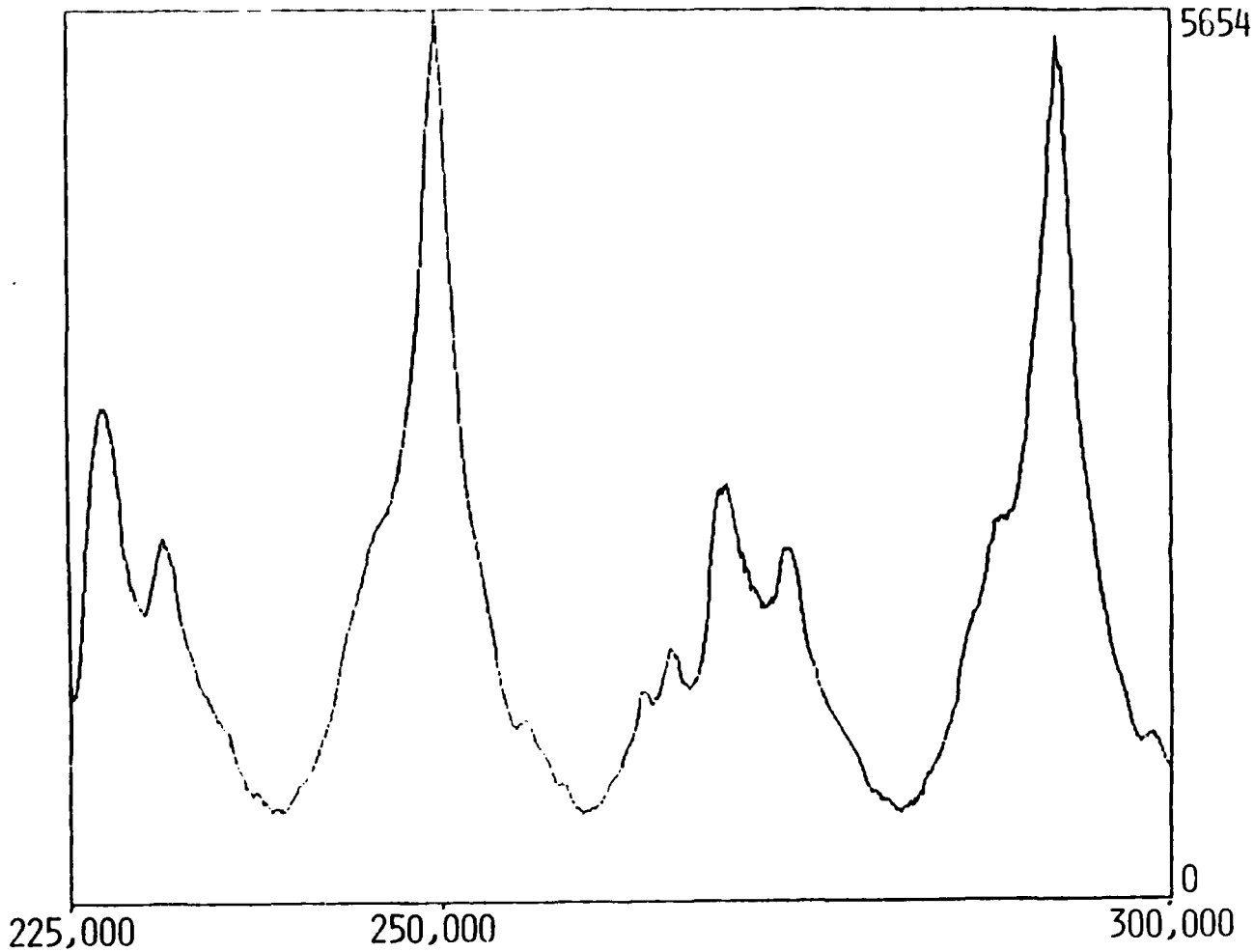

FIGURE 13

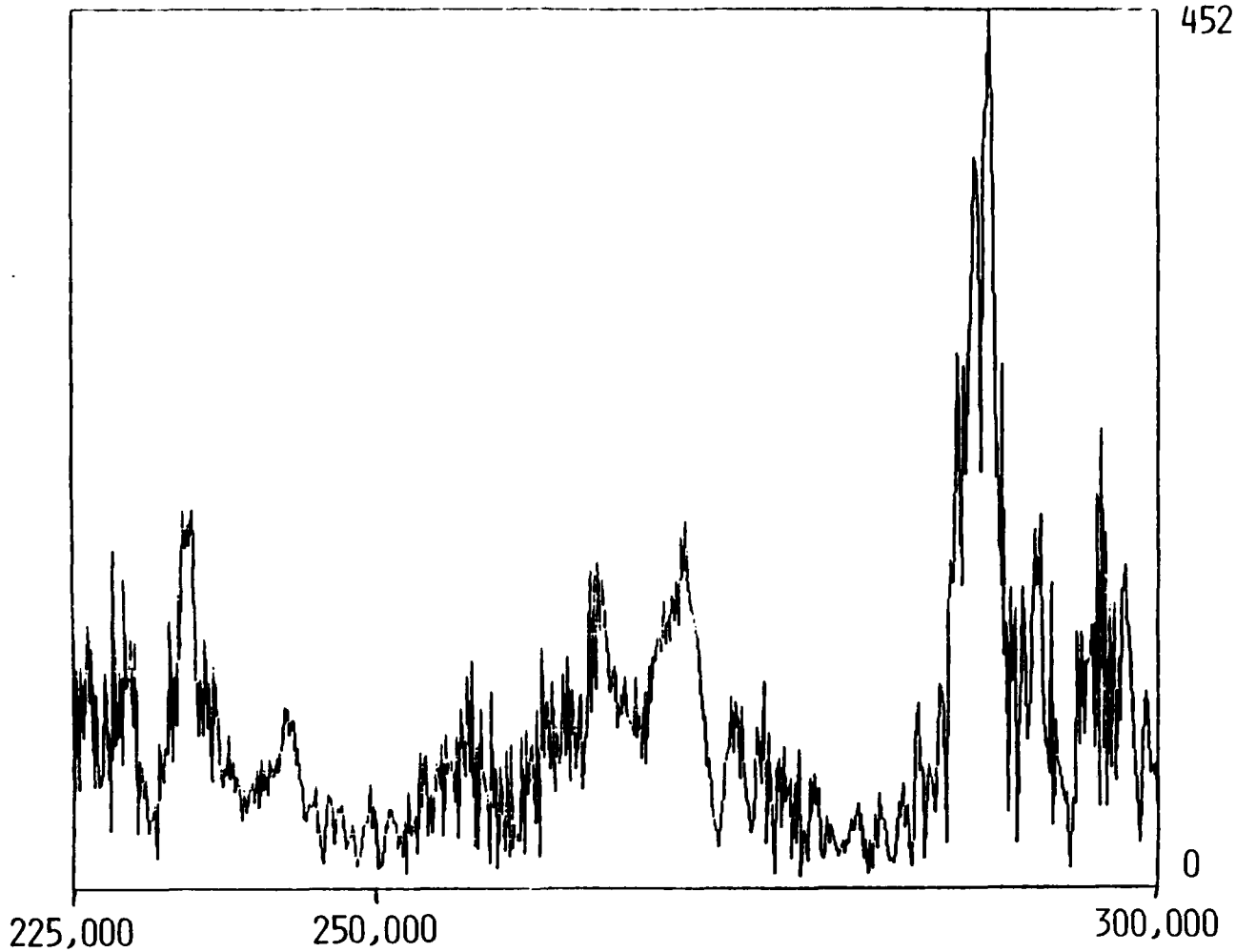

FIGURE 14

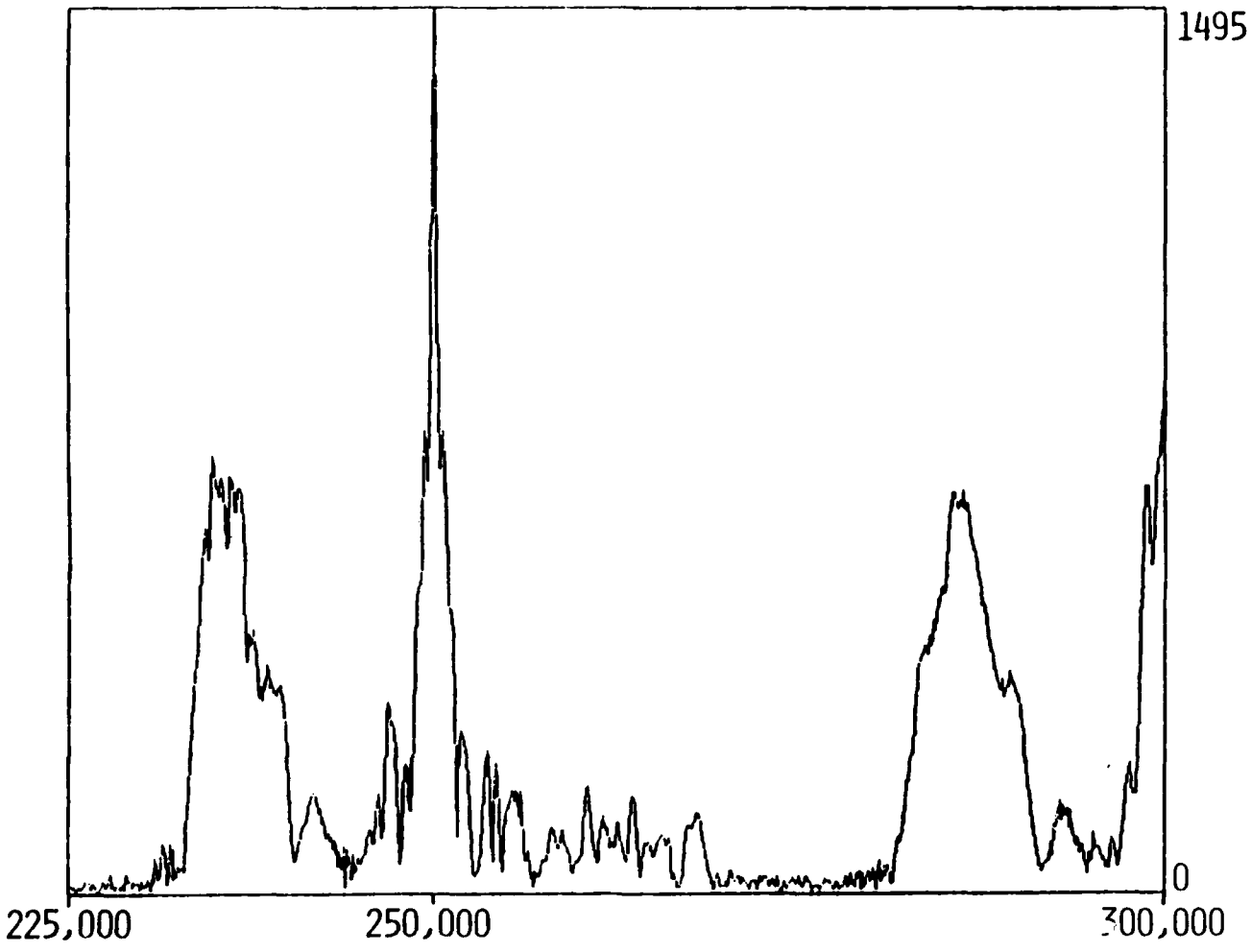

FIGURE 15

END
DATE
FILM
4-88
DTIC